Theta-Frequency Resonance in Hippocampal CA1 Neurons In Vitro Demonstrated by Sinusoidal Current Injection

L. STAN LEUNG AND HUI-WEN YU
Departments of Physiology and Clinical Neurological Sciences, The University of Western Ontario, London, Ontario N6A 5A5, Canada

Leung, L. Stan and Hui-Wen Yu. Theta-frequency resonance in hippocampal CA1 neurons in vitro demonstrated by sinusoidal current injection. *J. Neurophysiol.* 79: 1592–1596, 1998. Sinusoidal currents of various frequencies were injected into hippocampal CA1 neurons in vitro, and the membrane potential responses were analyzed by cross power spectral analysis. Sinusoidal currents induced a maximal (resonant) response at a theta frequency (3–10 Hz) in slightly depolarized neurons. As predicted by linear systems theory, the resonant frequency was about the same as the natural (spontaneous) oscillation frequency. However, in some cases, the resonant frequency was higher than the spontaneous oscillation frequency, or resonance was found in the absence of spontaneous oscillations. The sharpness of the resonance (Q), measured by the peak frequency divided by the half-peak power bandwidth, increased from a mean of 0.44 at rest to 0.83 during a mean depolarization of 6.5 mV. The phase of the driven oscillations changed most rapidly near the resonant frequency, and it shifted about 90° over the half-peak bandwidth of 8.4 Hz. Similar results were found using a sinusoidal function of slowly changing frequency as the input. Sinusoidal currents of peak-to-peak intensity of >100 pA may evoke nonlinear responses characterized by second and higher harmonics. The theta-frequency resonance in hippocampal neurons in vitro suggests that the same voltage-dependent phenomenon may be important in enhancing a theta-frequency response when hippocampal neurons are driven by medial septal or other inputs in vivo.

INTRODUCTION

The hippocampal theta rhythm of ~4–10 Hz is one of the most regular rhythms in the brain. It accompanies behavioral activation and likely plays an important role in the integrative and memory functions of the hippocampus (Bland and Colom 1993; Buzsaki et al. 1994).

Single hippocampal neurons in anesthetized animals showed membrane potential oscillations (MPOs) in phase with the theta electroencephalogram (EEG) (Fujita and Sato 1964; Konopacki et al. 1992; Leung and Yim 1986). The MPOs in vivo may consist of inhibitory (Fox 1989; Leung and Yim 1986) or excitatory postsynaptic potentials (Fujita and Sato 1964; Leung 1984; Nunez et al. 1987). Hippocampal theta rhythm is driven by neurons in the medial septal area (Petsche et al. 1962), but there is also evidence of rhythm generation within the hippocampus (Bland and Colom 1993) and the entorhinal cortex (Klink and Alonso 1993).

Theta-frequency MPOs were observed in single hippocampal CA neurons in vitro (Leung and Yim 1991), suggesting that single neurons may act as oscillators. An oscillator also may be driven to respond maximally at a resonant frequency, and the resonant frequency is just below the natural oscillation frequency for a linear system. However, resonance at the theta frequency has not been clearly demonstrated in hippocampal neurons (cf. Yu and Leung 1993). Garcia-Munoz et al. (1993), with sinusoidal currents of >100 pA, showed that hippocampal neurons responded more to 7 than 2 or 14 Hz, but responses were not quantified and resonance was not mentioned. Jahnsen and Karnup (1994) showed little resonance in power spectra of MPOs of hippocampal neurons driven by band-pass white noise.

In this study, a sharp resonance at the theta frequency was observed in many CA1 neurons driven by sinusoidal currents in vitro. A sinusoidal input is selected because hippocampal theta rhythm in vivo is almost sinusoidal (Leung and Yim 1986; Leung et al. 1982). Systems analysis using sinusoidal inputs is an established engineering technique (D'Azzo and Houpis 1966; Gwinn and Westervelt 1986). However, resonance in other central neurons was demonstrated by an impedance (Z) amplitude profile (ZAP) function input (Gutfreund et al. 1995; Puil et al. 1986), and thus the ZAP function (a sinusoidal function of slowly changing frequency) was also applied to CA1 neurons.

METHODS

Rat hippocampal slices were recorded at 32°C in vitro using 3 M K acetate micropipettes of impedance 80–150 MΩ (Leung and Yim 1991). The perfusate of pH 7.4 and saturated with 95% O_2-5% CO_2 consisted of (in mM) 124 NaCl, 5 KCl, 1.25 $NaH_2PO_4 \cdot H_2O$, 2 $MgSO_4 \cdot 7H_2O$, 2 $CaCl_2 \cdot 6H_2O$, 26 $NaHCO_3$, and 10 glucose. Neurons with resting membrane potential less than −55 mV and overshooting action potentials were selected. Input resistance was calculated as the maximal voltage deviation divided by the current during a hyperpolarizing current (0.2–0.4 nA) step of >150 ms duration. Steady-state responses were analyzed at >5 s after the onset of a sinusoidal or a step current. Sinusoidal currents (Fig. 1*B*) were applied by a function generator (Wavetek) at the bridge input of an Axon amplifier. A single microelectrode was used for both current injection and recording, with the bridge balanced. In the extracellular medium, the bridge was balanced when a step current caused no DC potential change. When recorded intracellularly, the bridge was balanced when a step current resulted in a smooth rise of the membrane potential. Bridge balance was checked and maintained every 1–2 min and after prolonged DC injection. Maximal capacitance compensation that did not cause ringing was used. Sinusoidal currents were injected both intra- and extracellularly. In the extracellular medium, the response to sinusoidal currents was small and not frequency selective. The ZAP function (Puil et al. 1986), generated electronically by voltage control generation, was described by A*sin $[2\pi f(t)*t]$

0022-3077/98 $5.00 Copyright © 1998 The American Physiological Society

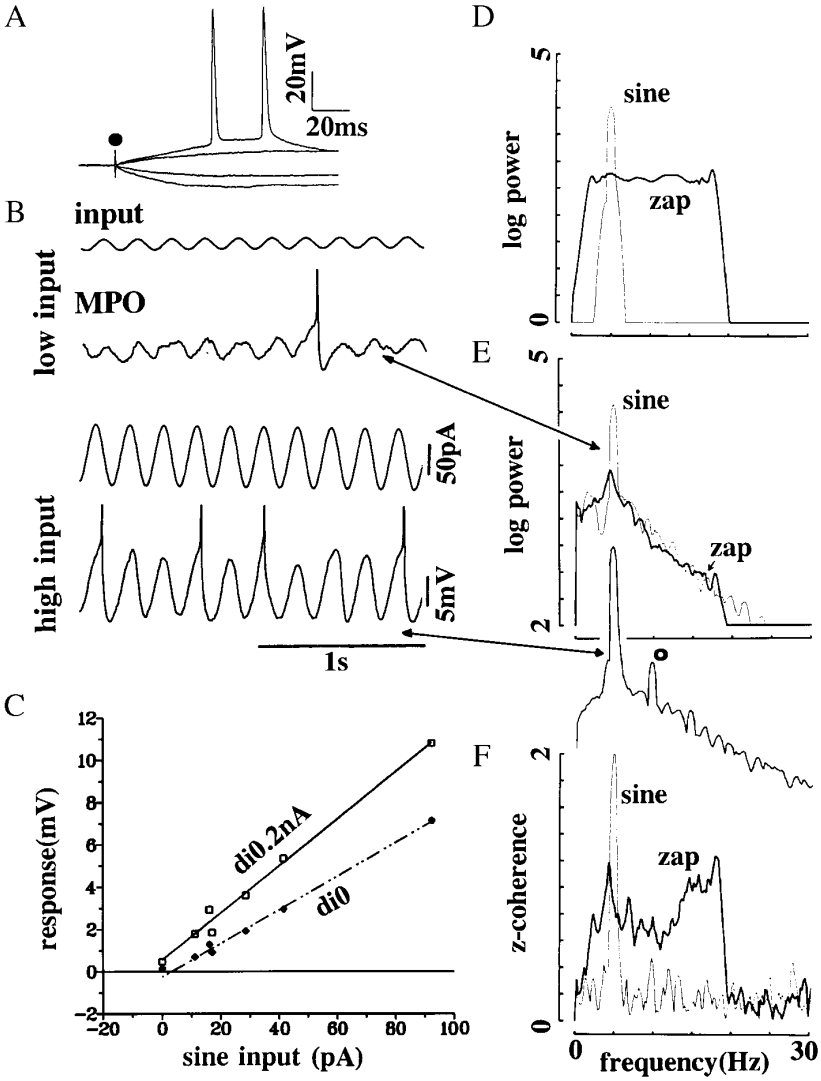

FIG. 1. CA1 neuron (*23807*) with different inputs. *A*: superimposed neuronal responses to 4 step currents (−0.4, −0.2, 0.2, and 0.3 nA) injected at the point of the artifact (●). Note depolarizing afterpotential and 2-spike burst response after 0.3-nA step. Resting membrane potential (RMP) was −65 mV. *B*: 2 pairs of traces, each consisting of an *top trace* (input at 5 Hz) and *bottom trace* (membrane potential oscillation, MPO) during low and high input; the neuron was depolarized to a mean potential of −56 mV during the 5-Hz input. *C*: plot of peak-to-peak response to 5-Hz input, linear regression lines ($R^2 > 0.98$) have slope 73 MΩ during rest (depolarizing current di 0 nA) and 102 MΩ during tonic depolarization (di 0.2 nA); the peak-to-peak response was derived from the average power spectrum. *D–F*: spectra during a 5-Hz sine (thin trace) and impedance amplitude profile (ZAP) function (thick trace) inputs, both of 18 pA peak-to-peak amplitude. *D*: input logarithmic power as a function of frequency. *E*: MPO response in logarithmic power (in arbitrary units): spectra corresponding to low (18 pA) and high (95 pA) sinusoidal inputs are indicated; ○, 2nd harmonic. *F*: coherence *z* transform (*z* coherence) represents the ''cross-correlation'' between input and response as a function of frequency (*z* coherence = 1 when cross-correlation coefficient = 0.76).

over the period $2T$, where A = amplitude, and $f(t) = f_o + (f_m - f_o)*t/T$ for time $t = 0$ to T and $f(t) = f_m - (f_m - f_o)*(t - T)/T$ for $t = T$ to $2T$. The frequency limits used were $f_o = 2$ Hz, $f_m = 20$ Hz, and $T = 5.5$ s.

Testing of the amplifier frequency response was performed by injecting sinusoidal currents into a RC model cell ($R = 50$ MΩ, RC = 25 ms) in series with a 100-MΩ electrode. Estimates of the impedance magnitude and phase of the model cell differed from the theoretical values by <0.1 log unit and <2°, respectively, for input frequency <30 Hz. Thus the amplifier circuitry (Fox 1982) did not significantly distort the recorded response. Changes in capacitance compensation (range <7 pF) was found to have negligible effects on the complex impedance of the model cell.

The input and the amplified potentials were sampled and digitized (12 bits) at 200 Hz. Cross-talk between two channels was less than −30 dB. Data segments of 1,024 points were subjected to fast Fourier transform, and autopower and cross-power (phase and coherence) spectra were calculated (Leung et al. 1982; Lopes da Silva 1993). The frequency bin was 0.19 Hz, but because of smoothing, only values every 0.98 Hz were independent of each other. A spectrum typically had >40 df to ensure reliability of the phase and power estimates (Lopes da Silva 1993). The sharpness of the resonance (Q) was estimated by the peak frequency divided by the half-peak power bandwidth (HBW) (Feynman et al. 1963). HBW was the frequency interval between the half-peak power (−3 dB power) points, which were estimated by interpolation of the linear power values.

In addition to digital filtering (Leung and Yim 1991), a single spike may be truncated manually at one to two points without editing the slower pre- and afterpotentials, which were indistinguishable from the MPOs. All neurons reported here had a firing rate of <3/s, and spike truncation may reduce power at >10 Hz but minimally affected the theta-frequency spectral estimates.

The experimental data in the complex plane (resistance and reactance) were fitted by an electrical model of the membrane in the range of 1–20 Hz (experimental data were available at 1, 3, 5, 7, 10, and 20 Hz). The fit indicator (FI) used was $FI = \Sigma_i (X_i - Y_i)^2/\Sigma_i (X_i - X_{mean})^2$, where Y_i = model value and X_i = data value, both at the ith frequency, X_{mean} = mean of the data values, and X_i, Y_i, and X_{mean} are complex numbers. The fit indicator FI essentially gives the mean error square as a fraction of the variance of the data.

RESULTS

A group of CA1 neurons studied in detail ($n = 20$) had resting membrane potential (RMP) −62 ± 1 mV (mean ± SE), spike height 78 ± 2 mV, and input resistance 37 ± 2 MΩ. All cells had afterpotentials characteristic of CA1 pyramidal cells (Fig. 1*A*).

The response to a small sinusoidal current was sinusoidal and imposed on the background activity (Fig. 1*B*). Power spectral analysis confirmed that the voltage output was at the same frequency and coherent with the input (Fig. 1, *D*–*F*). Increasing the input amplitude resulted in a slightly nonsinusoidal response (Fig. 1*B*), manifested as a second harmonic (○, Fig. 1*E*). In selected neurons, the second harmonic could be observed in MPO records that contained no spikes, suggesting that spike or afterpotentials do not cause the second harmonic. No subharmonics were observed.

The amplitude of the voltage response was approximately proportional to the amplitude of the small (<100 pA) sinusoidal input (Fig. 1*C*) in all five neurons tested. A larger slope impedance was found during tonic depolarization than rest (Fig. 1*C*). In the five neurons, the slope impedance during rest was 38.6 ± 11.3 MΩ, which increased 1.4 ± 0.1 times during tonic depolarization (of 8 ± 1 mV). The nonzero ''response'' at zero sinusoidal current was the background spontaneous activity.

In the example shown (Figs. 2 and 3*A*), the resonant frequencies during rest and tonic depolarization were both at 5 Hz, although the 5 Hz response was larger during tonic depolarization than rest. In other neurons, the resonant frequency was higher during tonic depolarization than rest (Table 1). The sharpness of the resonance *Q* was also higher during tonic depolarization than rest (Table 1). In the group of 20 CA1 neurons, we found a resonant frequency of 5.7 ± 0.4 Hz, HBW of 8.4 ± 1.4 Hz, and *Q* of 0.83 ± 0.07 (range 0.24–1.48) during a tonic depolarization of 6.5 ± 0.8 mV.

The sharpness of the frequency peak (*Q*) was compared between spectra obtained during sinusoidal current injection and during the ''spontaneous'' condition with no sinusoidal input. In the example shown (Fig. 3*A*), both spontaneous and driven activities peaked at ~5 Hz during tonic depolarization. However, at rest, a broad 5 Hz peak was found in the driven spectrum but no clear peak was found in the spontaneous spectrum (Fig. 3*A*). The latter spectrum was characteristic of a low-pass filter. In the group, during tonic depolarization, the resonant frequency (5.7 ± 0.4 Hz) was higher than the spontaneous peak frequency (4.7 ± 0.4 Hz)

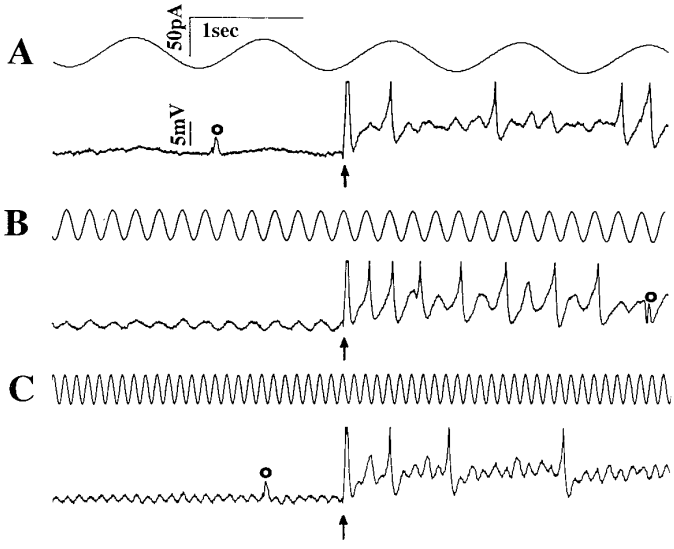

FIG. 2. *A*–*C*: sinusoidal current injection in a CA1 neuron (*23702*) at 1 Hz (*A*), 5 Hz (*B*), and 10 Hz (*C*); peak-to-peak current was 38 pA. ↑, application of step depolarizing current (0.2 nA). Each pair of traces consists of the input current *(top)* and membrane potential *(bottom)*. RMP was −58 mV. Spike tops were truncated. ○, infrequent spontaneous event.

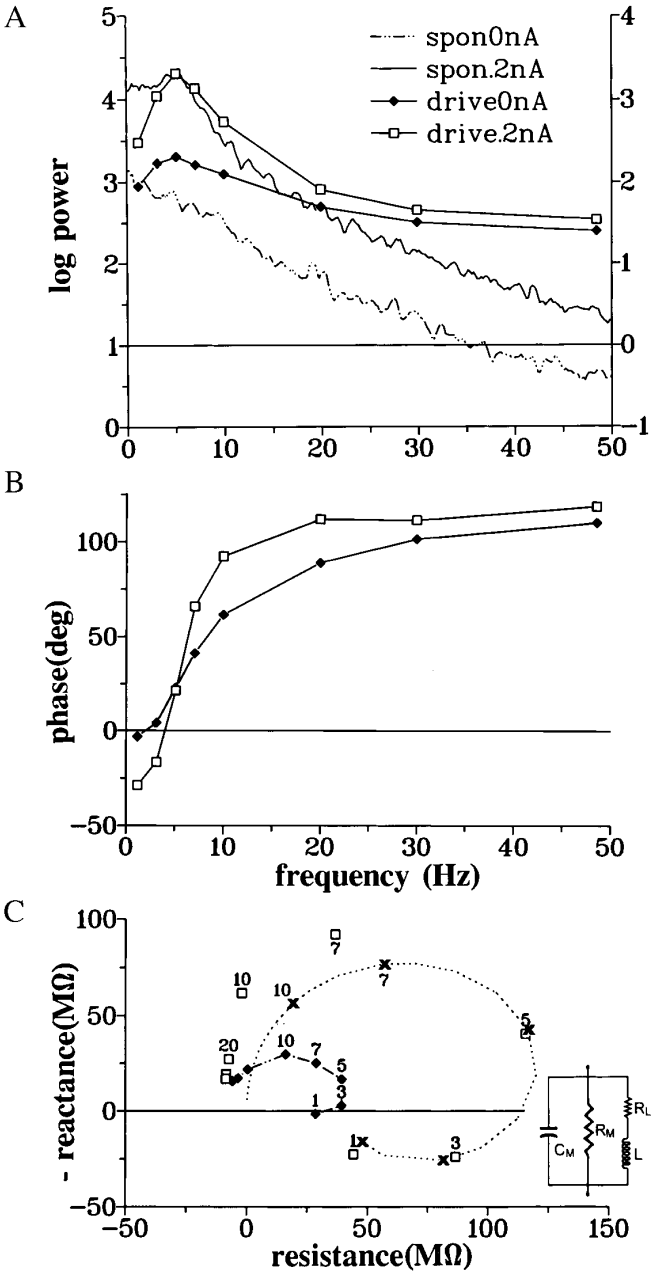

FIG. 3. Power and phase spectra of neuron shown in Fig. 2; symbol legend in *A* applies to *A*–*C* parts of the figure. *A*: spontaneous (spon; *right axis*) and sine-driven power spectra (– □ –, – ♦ –; *left axis*) during rest (0 nA) or tonic depolarization (di 0.2 nA). Frequency peak is sharper during depolarization than rest, and for driven than spontaneous activity. *B*: phase spectrum shows a steep phase change near the resonant frequency. *C*: plot of complex impedance of neuron during rest and tonic depolarization. An electrical model (*left inset*), using parameters R_m = 220 MΩ, C_m = 0.32 nF, R_L = 49 MΩ, and L = 3.74 MH, generates · · ·; X, response at a particular frequency (Hz). Model responses approximate the experimental data during depolarization (□), with larger deviations at 7 and 10 Hz than other frequencies. Fit indicator (METHODS) was 0.16. – – –, link of the experimental responses at rest (♦).

TABLE 1. *Spectral parameters during rest and tonic depolarization (depolarized) in 12 neurons evaluated in both rest and depolarized states*

	Sine Input		ZAP Input	
	Rest	Depolarized	Rest	Depolarized
Deviation from resting membrane potential, mV	0	6.7 ± 1.2*	0	6.7 ± 1.1†
Resonant frequency, Hz	4.5 ± 0.3	5.1 ± 0.5†	4.7 ± 1.0	5.3 ± 0.8
Half-peak bandwidth, Hz	15.2 ± 3.8	7.4 ± 1.4*	10.1 ± 3.6	7.5 ± 3.0†
Resonance sharpness	0.44 ± 0.07	0.83 ± 0.1*	0.57 ± 0.15	0.98 ± 0.18†

All 12 neurons were given a sinusoidal current but only 7 of the 12 neurons were given a sine wave with changing frequency [impedance amplitude profile (ZAP) input]. The parameters evaluated by sine and ZAP inputs were not different from each other in a given (rest or depolarized) state. $n = 12$ for sine input [10 rest (2 cells showed no resonant peak), 12 depolarized]; $n = 7$ for ZAP input [5 rest (2 cells showed no resonant peak); $n = 7$ depolarized]. * $P < 0.01$, † $P < 0.05$, paired Wilcoxon, rest value different from depolarized value.

($P < 0.05$, paired Wilcoxon, $n = 20$). Q was not significantly different between spontaneous and driven spectra obtained during tonic depolarization. In 12 neurons at rest, a frequency peak was observed in 10 neurons during sinusoidal driving (Table 1) but only in 5 neurons in the spontaneous spectrum, i.e., a frequency peak occurred more reliably with than without sinusoidal driving ($P < 0.05$, χ^2).

The phase of the driven activities changed rapidly at low frequency, and most rapidly at the resonant frequency (Fig. 3, *B* and *C*). The phase change with frequency was faster for a high than a low Q (Fig. 3*B*). With tonic depolarization, a phase shift of 87 ± 9° ($n = 20$) was observed over the interval of the half-peak-bandwidth.

Because resonance has been attributed to a phenomenological inductance in the membrane (Mauro et al. 1970; Puil et al. 1986), we have attempted to see if a similar electrical model may approximate the theta-frequency resonance of CA1 neurons. The proposed electrical model consists of membrane resistance R_m, capacitance C_m, and a inductance (L) plus resistance (R_L) in parallel (Fig. 3*C*) (Crawford and Fettiplace 1981; Puil et al. 1986). The experimental and model-generated data are drawn in the complex impedance plot (Fig. 3*C*). In the example shown, the model approximates the experimental responses well at <7 Hz but less well at the falling phase of the resonant peak (7–10 Hz). In eight neurons, the fit indicator (METHODS) averaged 0.24 ± 0.04 ($n = 8$). The estimated model parameters were natural frequency $f_p = 1/(2\pi\sqrt{LC_m}) = 3.87 \pm 0.48$ Hz, $R_m = 358 \pm 143$ MΩ, $R_L = 77 \pm 16$ MΩ, and $C_m = 0.37 \pm 0.08$ nF (all $n = 8$).

In seven neurons given a ZAP input (<50 pA peak-to-peak amplitude), the resulting Q and HBW estimates did not differ significantly from those using sine inputs (Table 1). The ZAP input had a relatively flat power between 3 and 18 Hz (Fig. 1*D*), but the response (Fig. 1*E*) showed a peak at 4.5 Hz. For the low-amplitude ZAP input used, the response outside of the theta-frequency range was small.

DISCUSSION

This is an original study of the resonant response of single hippocampal neurons. For small signals, the membrane responses obeyed the principles of proportionality and superposition, i.e., the system may be regarded as linear, and thus similar results were found using ZAP and sinusoidal inputs. However, deviation from linearity was found for currents >100 pA, as shown by responses with the second and higher harmonics (Fig. 1). This type of nonlinearity rarely has been addressed before, and harmonics cannot be revealed by ZAP inputs. The harmonics of the MPOs may contribute to the harmonics of the theta rhythm in behaving rats (Leung et al. 1982).

The theoretical prediction that the resonant frequency is near the natural oscillation frequency mainly is confirmed. However, two findings are not expected. First, the resonant frequency was slightly higher than the spontaneous (presumed natural) frequency, and second, near rest, resonance may be observed without clear spontaneous oscillations. These two results may be attributed partly to a voltage-dependent nonlinearity. Because a slight depolarization may turn on oscillations, a small sinusoidal input may be expected to add to the root-mean–square voltage and enhance the resonant response of the neuron. Similarly, Puil et al. (1986) found that the resonant frequency was typically higher than the predicted natural frequency of trigeminal motoneuron, and Gutfreund et al. (1995) inferred spontaneous and driven oscillations had different requirements in frontal cortex neurons.

A persistent Na^+ current and a slow K^+ current were important for MPOs in frontal cortical neurons (Gutfreund et al. 1995) as well as for the spontaneous hippocampal MPOs (Leung and Yim 1991) and their resonance (unpublished data). A phenomenological membrane inductance has been inferred for other neurons (Mauro et al. 1970; Puil et al. 1986), and a similar second-order model with inductance (Fig. 3*C*) can account for the main characteristics of the complex impedance (i.e., both amplitude and phase) near the resonant peak of CA1 neurons.

A rapid phase change near the resonant frequency and a ~90° shift across the HBW are typical of an oscillatory system (D'Azzo and Houpis 1966). A voltage-dependent mechanism partly controls the theta-frequency phase shift, e.g., the phase of the driven MPOs at 7–10 Hz shifted ~30° from rest to tonic depolarization (Fig. 3*B*). The latter mechanism may explain in part the progressive increase in the theta-frequency phase shift between unit firing and theta EEG as a rat crossed a particular location in space (O'Keefe and Reece 1993). Other mechanisms, e.g., two theta inputs of different phases (Leung 1984) or asynchronous field and cellular oscillators, also may be involved.

The present results are relevant to the generation of the hippocampal theta rhythm in vivo. While the in vitro rhythms

were mainly studied near 32°C, preliminary results have indicated no essential difference between the MPOs at 32 and 37°C (normal body temperature). In vivo, theta-frequency driving of the hippocampus is derived from the medial septal and other neurons (Bland and Colom 1993; Petsche et al. 1962), but intrinsic voltage-dependent mechanisms may enhance or depress the driven response. We show here that the sharpness of the resonance and the resonant frequency were increased by tonic depolarization, and a resonant response may be found even when spontaneous oscillations were not apparent. In conclusion, this study emphasizes that a single neuron can modulate its own rhythmicity and that local (as well as extrinsic) factors may regulate neuronal recruitment and synchronization, which may be important during hippocampal functions.

We thank B. Shen, C. Wu, K. Wu, and D. Zhao for technical assistance, C. Yim for programming, R. Harshman for discussion on statistics, and K. Canning for reading the manuscript.

The research was supported by the National Sciences and Engineering Research Council (Canada).

Address for reprint requests: L. S. Leung, Dept. of Clinical Neurological Sciences, University Campus, London Health Science Centre, The University of Western Ontario, London, Ontario N6A 5A5, Canada.

Received 4 March 1997; accepted in final form 17 November 1997.

REFERENCES

BLAND, B. H. AND COLOM, L. V. Extrinsic and intrinsic properties underlying oscillation and synchrony in limbic cortex. *Prog. Neurobiol.* 41: 157–208, 1993.

BUZSAKI, G., BRAGIN, A., CHROBAK, J. J., NADASDY, Z., SIK, A., HSU, M., AND YLINEN, A. Oscillatory and intermittent synchrony in the hippocampus: relevance to memory trace formation. In: *Temporal Coding in the Brain*, edited by G. Buzsaki, R. Llinas, W. Singer, A. Bethoz, and T. Christian. New York: Springer-Verlag, 1994, p. 145–172.

CRAWFORD, A. C. AND FETTIPLACE, R. Non-linearities in the responses of turtle hair cells. *J. Physiol. (Lond.)* 315: 317–338, 1981.

D'AZZO, J. J. AND HOUPIS, C. H. *Feedback Control System Analysis and Synthesis.* New York: McGraw, 1966.

FEYNMAN, R. P., LEIGHTON, R. B., AND SANDS, M. *The Feynman Lectures on Physics.* Reading, MA: Addison-Wesley, 1963.

FOX, S. E. Solutions to three capacitance problems in intracellular single-electrode bridge amplifiers. *IEEE Trans. Biomed. Eng.* 29: 662–666, 1982.

FOX, S. E. Membrane potential and impedance changes in hippocampal pyramidal cells during theta rhythm. *Exp. Brain Res.* 77: 283–294, 1989.

FUJITA, Y. AND SATO, T. Intracellular records from hippocampal pyramidal cells in rabbit during theta rhythm activity. *J. Neurophysiol.* 27: 1011–1025, 1964.

GARCIA-MUNOZ, A., BARRIO, L. C., AND BUNO, W. Membrane potential oscillations in CA1 hippocampal pyramidal neurons in vitro—intrinsic rhythms and fluctuations entrained by sinusoidal injected current. *Exp. Brain Res.* 97: 325–333, 1993.

GUTFREUND, Y., YAROM, Y., AND SEGEV, I. Subthreshold oscillations and resonant frequency in guinea-pig cortical neurons: physiology and modelling. *J. Physiol. (Lond.)* 483: 621–640, 1995.

GWINN, E. G. AND WESTERVELT, R. M. Fractal basin boundaries and intermittency in the driven damped pendulum. *Physiol. Rev. A.* 33: 4143–4155, 1986.

JAHNSEN, H. AND KARNUP, S. A spectral analysis of the integration of artificial synaptic potentials in mammalian central neurons. *Brain Res.* 666: 9–20, 1994.

KLINK, R. AND ALONSO, A. Ionic mechanisms for the subthreshold oscillations and differential electroresponsiveness of medial entorhinal cortex layer-II neurons. *J. Neurophysiol.* 70: 144–157, 1993.

KONOPACKI, J., BLAND, B. H., COLOM, L. V., AND ODDIE, S. D. In vivo intracellular correlates of hippocampal formation theta-on and theta-off cells. *Brain Res.* 586: 247–255, 1992.

LEUNG, L. S. Model of gradual phase shift of theta rhythm in the rat. *J. Neurophysiol.* 52: 1051–1065, 1984.

LEUNG, L. S., LOPES DA SILVA, F. H., AND WADMAN, W. J. Spectral characteristics of hippocampal EEG in the freely moving rat. *Electroencephalogr. Clin. Neurophysiol.* 54: 203–219, 1982.

LEUNG, L. S. AND YIM, C. Y. Intracellular records of theta rhythm in hippocampal CA1 cells of the rat. *Brain Res.* 367: 323–327, 1986.

LEUNG, L. S. AND YIM, C. Y. Intrinsic membrane potential oscillations in hippocampal neurons in vitro. *Brain Res.* 553: 261–274, 1991.

LOPES DA SILVA, F. H. EEG analysis: theory and practice. In: *Electroencephalography* (3rd ed.), edited by E. Niedermeyer and F. H. Lopes da Silva. Baltimore, MD: Williams and Wilkins, 1993, p. 1097–1123.

MAURO, A., CONTI, F., DODGE, F., AND SCHOR, R. Subthreshold behavior and phenomenological impedance of the squid giant axon. *J. Gen. Physiol.* 55: 497–523, 1970.

NUNEZ, A., GARCIA-AUSTT, E., AND BUNO, W., JR. Intracellular θ-rhythm generation in identified hippocampal pyramids. *Brain Res.* 416: 289–300, 1987.

O'KEEFE, J. AND REECE, M. L. Phase relationship between hippocampal place units and the EEG theta rhythm. *Hippocampus* 3: 317–330, 1993.

PETSCHE, H., STUMPF, C., AND GOGOLAK, G. The significance of the rabbit's septum as a relay station between the midbrain and the hippocampus. I. The control of hippocampal arousal activity by the septum cells. *Electroencephalogr. Clin. Neurophysiol.* 14: 202–211, 1962.

PUIL, E., GIMBARZEVSKY, B., AND MIURA, R. M. Quantification of membrane properties of trigeminal root ganglion neurons in guinea pigs. *J. Neurophysiol.* 55: 995–1016, 1986.

YU, H. W. AND LEUNG, L. S. Oscillatory driving of hippocampal CA1 cells in vitro. *Soc. Neurosci. Abstr.* 19: 356, 1993.